Received: 25 February 2021 | Revised: 9 June 2021 | Accepted: 10 June 2021

DOI: 10.1111/epi.16979

Epilepsia®

FULL-LENGTH ORIGINAL RESEARCH

Gut metabolite S-equol ameliorates hyperexcitability in entorhinal cortex neurons following Theiler murine encephalomyelitis virus-induced acute seizures

Allison Gallucci[1,2] | **Dipan C. Patel**[3] | **K'Ehleyr Thai**[1,2] | **Jonathan Trinh**[4] | **Rosalie Gude**[2] | **Devika Shukla**[5] | **Susan L. Campbell**[2,5]

[1]Graduate Program in Translational Biology Medicine and Health, Virginia Tech, Roanoke, Virginia, USA

[2]Animal and Poultry Sciences, Virginia Polytechnic Institute and State University, Blacksburg, Virginia, USA

[3]Fralin Biomedical Research Institute, Virginia Polytechnic Institute and State University, Roanoke, Virginia, USA

[4]University of South Alabama College of Medicine, Mobile, Alabama, USA

[5]School of Neuroscience, Virginia Polytechnic Institute and State University, Blacksburg, Virginia, USA

Correspondence
Susan L. Campbell, Animal and Poultry Sciences, 2200 Litton Reaves Hall, Virginia Polytechnic and State University, Blacksburg, VA 24061, USA.
Email: susanc08@vt.edu

Funding information
College of Agricultural and Life Sciences at Virginia Tech; School of Neuroscience at Virginia Tech; Virginia Tech Insitute for Critical Technology and Applied Science (ICTAS)

Abstract

Objective: A growing body of evidence indicates a potential role for the gut–brain axis as a novel therapeutic target in treating seizures. The present study sought to characterize the gut microbiome in Theiler murine encephalomyelitis virus (TMEV)-induced seizures, and to evaluate the effect of microbial metabolite S-equol on neuronal physiology as well as TMEV-induced neuronal hyperexcitability ex vivo.

Methods: We infected C57BL/6J mice with TMEV and monitored the development of acute behavioral seizures 0–7 days postinfection (dpi). Fecal samples were collected at 5–7 dpi and processed for 16S sequencing, and bioinformatics were performed with QIIME2. Finally, we conducted whole-cell patch-clamp recordings in cortical neurons to investigate the effect of exogenous S-equol on cell intrinsic properties and neuronal hyperexcitability.

Results: We demonstrated that gut microbiota diversity is significantly altered in TMEV-infected mice at 5–7 dpi, exhibiting separation in beta diversity in TMEV-infected mice dependent on seizure phenotype, and lower abundance of genus *Allobaculum* in TMEV-infected mice regardless of seizure phenotype. In contrast, we identified specific loss of S-equol-producing genus *Adlercreutzia* as a microbial hallmark of seizure phenotype following TMEV infection. Electrophysiological recordings indicated that exogenous S-equol alters cortical neuronal physiology. We found that entorhinal cortex neurons are hyperexcitable in TMEV-infected mice, and exogenous application of microbial-derived S-equol ameliorated this TMEV-induced hyperexcitability.

Significance: Our study presents the first evidence of microbial-derived metabolite S-equol as a potential mechanism for alteration of TMEV-induced neuronal excitability. These findings provide new insight for the novel role of S-equol and the gut–brain axis in epilepsy treatment.

KEYWORDS
electrophysiology, gut–brain axis, seizures, S-equol, TMEV

1 | INTRODUCTION

Epilepsy is one of the most common chronic neurological disorders worldwide, with a global incidence of ~5 million people each year.[1] People with epilepsy suffer from social stigma, debilitating comorbidities, and premature death.[1] The most common cause of epilepsy worldwide is central nervous system (CNS) infection; however, there are no antiseizure medications that specifically target infection-induced seizures. The bacteria that inhabit the mucosal surfaces of the body, termed the microbiota, are known to modulate a wide variety of peripheral diseases and have recently been implicated in multiple neural disorders.[2–4] In epilepsy, adults and children with drug-resistant seizures have altered microbiomes compared to adults with seizures that respond to drug therapy and age-matched healthy controls, respectively.[5,6] Additionally, probiotic supplementation has been shown to improve seizure burden in adults, children, and rodents with seizures that are refractory to drug treatment,[7–9] although a relative paucity of studies as well as generally correlative experimental designs make firm conclusions on the role of the gut–brain axis in seizures difficult to draw.[10] Therefore, there is a gap in our knowledge of specific mechanisms by which gut microbes modulate seizures, which in turn impedes efforts to develop potential gut–brain axis therapeutics in epilepsy.

S-equol is a metabolite produced exclusively by the metabolism of soy isoflavones by the gut microbiota.[11] It is highly available in serum in its free form[12] and crosses the blood–brain barrier.[13] Importantly, S-equol is neuroprotective against glutamate excitotoxicity in cultured hippocampal neurons,[14] indicating a potential role in protecting against hippocampal excitotoxicity and cell death commonly found in epilepsy patients and rodent models.[15,16] Although multiple studies point to neuroprotective effects, no studies have yet examined the role of microbially derived S-equol in neuronal physiology.

In the present study, we show significant alterations in the gut microbiome of C57BL/6J mice following Theiler murine encephalomyelitis virus (TMEV) infection. Additionally, we identify loss of key S-equol-producing microbial taxa associated with TMEV-induced seizure phenotype relative to TMEV-infected mice that do not display seizures. We demonstrate the ability of exogenous S-equol to alter neuronal physiology in a concentration- and time-dependent manner. Lastly, we also show marked increase in excitability of entorhinal cortex (ECTX) neurons in TMEV-infected mice, and demonstrate the ability of microbially derived S-equol to ameliorate TMEV-induced hyperexcitability. Collectively, our results indicate a central role for a microbially derived metabolite in regulating neuronal excitability and propose a mechanistic link between the gut–brain axis and TMEV-induced seizures.

Key Points

- TMEV infection in C57BL/6J mice leads to altered gut microbiota at 5–7 dpi
- Loss of S-equol-producing bacteria is a microbial hallmark of seizure phenotype following TMEV infection
- Exogenous S-equol alters cortical neuronal physiology in a concentration- and time-dependent manner
- ECTX neurons from TMEV-infected mice are hyperexcitable compared to PBS-injected controls, and exogenous application of S-equol ameliorates TMEV infection-induced ECTX hyperexcitability

2 | MATERIALS AND METHODS

2.1 | Animals

Animals were housed and handled according to the guidelines of the National Institutes of Health Committee on Laboratory Animal Resources. Prior approval of the Virginia Polytechnic Institute and State University institutional animal care and use committee was obtained for all experimental protocols. All efforts were made to minimize animal pain. C57BL/6J mice (stock #000664) aged 5–6 weeks were purchased from the Jackson Laboratory. Mice were allowed to acclimatize for at least 7 days prior to experiments. Mice were provided chow (Envigo 2918) and water ad libitum and kept in a facility providing 12-h light/dark cycle. TMEV-infected mice were housed separately from phosphate-buffered saline (PBS)-injected mice due to the infectious nature of the virus; however, all TMEV-infected mice were housed together regardless of seizure phenotype. All the experiments included almost equal numbers of male and female mice.

2.2 | TMEV infection and seizure monitoring

Six- to 8-week-old C57BL/6J mice were anesthetized with isoflurane and injected intracortically with 2×10^5 plaque-forming units of the Daniels strain of TMEV or PBS as previously described.[17] Acute behavioral seizures were induced twice daily 2–7 days postinfection (dpi) by shaking the cage to agitate the mice. Behavioral seizure intensity was graded using the following modified Racine seizure scale: Stage 1, mouth and facial movements; Stage 2, head nodding; Stage 3, forelimb clonus; Stage 4, forelimb clonus and rearing on hind limbs; Stage 5, forelimb clonus, rearing, and falling; and Stage 6, intense running, jumping, repeated falling, and severe clonus.[18] Across

cohorts, up to 80% of mice infected with TMEV exhibited at least one behavioral seizure on this scale. Seizure phenotype was defined as the presence of at least one handling-induced behavioral seizure of any intensity during monitoring.

2.3 | Fecal collection and DNA isolation

Fecal pellets were dissected from the distal colon of TMEV-infected and PBS-treated control mice 5–7 dpi using clean tweezers immediately following cervical dislocation. Pellets were stored in DNA-free Eppendorf tubes (Cat. No. 022600028) at −80°C.

Mouse fecal DNA was isolated using the DNA Fecal/Soil Microbe Miniprep Kit (Zymo Research) according to the manufacturer's instructions. DNA was quantified, and samples were stored at −80°C until sequenced.

2.4 | 16S sequencing and analysis

The universal primers 515F and 926R were chosen to amplify the V4–V5 region of the 16S rRNA gene following the Earth Microbiome Project protocol (https://www.earthmicrobiome.org/). The polymerase chain reaction (PCR) reaction mixture included 13.0 µl of PCR-grade water, 1.0 µl of template DNA, 10 µmol·L^{-1} of each primer, and 10.0 µl of 5PRIME HotMasterMix (2×; Quantabio). Samples were amplified in duplicate under the following thermocycler conditions: 94°C for 3 min for initial denaturing, then 35 cycles of 94°C for 45 s, 50°C for 60 s, and 72°C for 90 s. A final elongation step occurred at 72°C for 10 min followed by a hold at 4°C. After pooling duplicates, amplicons were visualized on a 2% agarose gel and quantitated on a Qubit fluorometer (Thermo Fisher Scientific). Normalization was performed based on Qubit results, and amplicons were purified on a Pippin Prep (Sage Science) targeting a 520-bp range. This pool was quantitated using quantitative PCR. Amplicons were loaded at 9.5 pmol·L^{-1} and sequenced using the MiSeq v3 600-cycle kit on the Miseq platform (Illumina). Sequencing yielded 19.6 million paired-end reads. Quality scores were within Illumina specifications.

Sequencing data were analyzed with QIIME2 v2019.10.[19] Forward and reverse reads were quality filtered, trimmed, and joined with DADA2; DADA2 was also used to denoise joined reads to amplicon sequence variants (ASVs; via q2-dada2). ASVs were aligned to a phylogenetic tree using an insertion method to the Greengenes reference database (via q2-fragment-insertion-sepp). Differential abundance was measured using analysis of compositions of microbiomes (ANCOM).[20] Linear discriminant effect size analysis (LEfSe) was performed with default parameters.[21] Operational taxonomic unit tables generated in QIIME were assigned linear discriminant analysis (LDA) scores and graphed utilizing the Galaxy web application.

2.5 | Slice preparation

Coronal slices for naïve experiments were prepared as reported previously.[22] Briefly, male naïve C57BL/6 mice were decapitated, and their brains were quickly removed and immersed in ice-cold cutting solution containing (in mmol·L^{-1}) 135 N-methyl-d-glucamine (NMDG), 1.5 KCl, 1.5 KH2PO4, 23 choline bicarbonate, 25 d-glucose, .5 CaCl2, and 3.5 MgSO4 (Sigma-Aldrich). Three-hundred-micrometer coronal brain slices were made and recovered for 40–60 min in oxygenated recording solution containing (in mmol·L^{-1}) 125 NaCl, 3 KCl, 1.25 NaH2PO4, 25 NaHCO3, 2 CaCl2, 1.3 MgSO4, and 25 d-glucose at 32°C and maintained at room temperature before recordings.

For horizontal slices for ECTX recordings, male and female TMEV-infected or PBS-injected mice were anesthetized with ketamine/xylazine at 5–7 dpi and transcardially perfused with ice-cold cutting solution containing (in mmol·L^{-1}) 92 NMDG, 2.5 KCl, 1.2 NaH_2PO_4, 30 $NaHCO_3$, 20 hydroxyethylpiperazine ethane sulfonic acid (HEPES), 25 D-(+)-glucose, 5 sodium-L-ascorbate, 3 sodium pyruvate, .5 $CaCl_2$, and 10 $MgCl_2$ for 1.5 min before quick extraction of the brain. Horizontal brain slices (300 µmol·L^{-1}) were prepared by following the NMDG protective recovery method.[23] Briefly, the brain slices were allowed to recover from slicing insult in the cutting solution at 32°C for a total of 25 min. During this recovery period, sodium concentration of the incubation solution was gradually increased from about 40 mmol·L^{-1} present in the cutting solution to 128 mmol·L^{-1} by adding NaCl solution in the incubation chamber every 5 min. Subsequently, the slices were transferred to the holding artificial cerebrospinal fluid (ACSF) containing (in mol·L^{-1}) 92 NaCl, 2.5 KCl, 1.2 NaH_2PO_4, 30 $NaHCO_3$, 20 HEPES, 25 D-(+)-glucose, 5 sodium-L-ascorbate, 3 sodium pyruvate, 2 $CaCl_2$, and 2 $MgCl_2$ at room temperature. The slices were incubated in the holding ACSF for at least 1 h before being used for electrophysiological recordings. All electrophysiological recordings were performed in the recording ACSF containing (mol·L^{-1}) 125 NaCl, 3 KCl, 1.25 NaH_2PO_4, 25 $NaHCO_3$, 5 HEPES, 12.5 D-(+)-glucose, 2 $CaCl_2$, and 2 $MgCl_2$ with either 1 µmol·L^{-1} S-equol (Cayman Chemicals) or equal dimethylsulfoxide concentration (<.05%).

2.6 | Electrophysiology

Individual brain slices were transferred to a recording chamber and continuously perfused (4 ml/min) with oxygenated recording solution. Whole-cell recordings were conducted using

borosilicate glass capillaries (KG-33 glass; Garner Glass) and filled with internal solution containing (in mol·L^{-1}) 134 K-gluconate, 1 KCl, 10 HEPES, 2 Mg-adenosine triphosphate; .2 Na-guanosine triphosphate, and .5 ethyleneglycoltetraacetic acid. The pH was set to 7.3 with KOH, and the osmolality was measured (~290 mOsm/kg). All recordings were performed at 32 ± 1°C. Individual cells were visualized using an Axioscope (Carl Zeiss) microscope equipped with Nomarski optics with a ×40 water-immersion objective lens. Tight seals were made using electrodes with a 3–5-MΩ open-tip resistance. Signals were acquired from pyramidal ECTX cells and principal cortical neurons with an Axopatch 1B amplifier (Molecular Devices), controlled by Clampex 11 software via a Digidata 1440 interface (Molecular Devices). Action potential threshold current and input–output curves were calculated as described previously.[24] For the experiments involving S-equol, slices were preincubated in 1 μmol·L^{-1} S-equol (Cayman Chemicals) for at least 2 h before recordings.

2.7 | Statistics

Alpha diversity values were calculated with observed features and evenness metrics. Beta diversity analyses were calculated with weighted and unweighted UniFrac distance. LDA score for LEfSe analysis was performed on differential abundance tables generated with QIIME. Microbiome differences between experimental groups were assessed using ANCOM analysis and Kruskal–Wallis *H*-tests with Dunn multiple comparisons correction. All *p*-values for Kyoto Encyclopedia of Genes and Genomes pathways are false discovery rate adjusted. Statistical details of experiments are mentioned in the figure legends. Data are sufficiently normally distributed and variance within groups is sufficiently small for data to be used for parametric tests when specified. Experimental designs with two treatment groups were analyzed by two-tailed unpaired *t*-tests. Welch correction was applied where variances of both the groups were statistically different. Experimental designs with more than two groups were analyzed using one-way analysis of variance (ANOVA) or two-way ANOVA followed by Tukey or Sidak post hoc multiple comparison tests where specified. Data analysis was performed using GraphPad Prism 8.0, Microsoft Excel, and Origin 2016 (OriginLab).

3 | RESULTS

3.1 | TMEV infection and seizure phenotype are associated with altered gut microbiota diversity

We first characterized the gut microbiota of C57BL/6J mice infected with TMEV. Typically, TMEV infection induces acute seizures at 3–10 dpi in approximately 50%–65% of infected mice.[25] Analysis of fecal microbiota of TMEV-injected and PBS-injected age-matched mice at 5–7 dpi (Figure 1A) showed no difference in alpha diversity richness (observed features) across any group (PBS, mean = 143 ± 14.4; TMEV–no seizure, 140.5 ± 9.7; TMEV–seizure, 127.9 ± 10; not significant [ns], Kruskal–Wallis test; Figure 1B). Although alpha diversity measures of evenness (Pielou) revealed a trend toward lower diversity in TMEV-infected mice with seizure phenotypes compared to both PBS-injected controls and TMEV-infected mice that did not develop seizures, the result was not significant (PBS, mean = .54 ± .03; TMEV–no-seizure, .53 ± .03; TMEV–seizure, .44 ± .4; $p = .08$, Kruskal–Wallis test; Figure 1C). Interestingly, beta diversity measured by weighted UniFrac distance showed significant separation of all three experimental groups, indicating distinct communities of microbes across all three experimental conditions ($p = .001$, permutational multivariate ANOVA [PERMANOVA]; Figure 1D). Taken together, these findings indicate that TMEV infection and seizure phenotype following TMEV infection are associated with altered gut microbiome diversity.

3.2 | Selective alteration in microbial taxa in TMEV-infected mice

As diversity analyses revealed separation of all experimental groups, we examined which taxonomies were altered in TMEV-infected mice. Regardless of experimental condition, the microbiomes of all mice in this study are dominated by Firmicutes and Bacteroidetes phyla (Figure 2A). We found no difference in Firmicutes/Bacteroidetes ratio across any experimental group (PBS, mean = 2.33 ± .5; TMEV–no seizure, 1.14 ± .3; TMEV–seizure, 3.19 ± .8; n.s., Kruskal–Wallis test; Figure 2B). We next performed ANCOM analysis via QIIME2 to examine alterations in the composition of microbes across our experimental groups.[26] Regardless of seizure phenotype, mice infected with TMEV displayed lower abundances of *Allobaculum* (PBS, mean = .250 ± .071; TMEV–no seizure, .037 ± .018; TMEV–seizure, .019 ± .013; null hypothesis rejected, ANCOM; Figure 2C).

To further identify key alterations in microbial taxa following TMEV infection, the well-established feature analysis LEfSe, an algorithm that employs LDA to identify differential features among experimental groups, was used.[21] Figure 2D shows the clades that best describe PBS-injected controls compared to TMEV-infected mice. Again, loss of genus *Allobaculum* was identified as a key biomarker of TMEV infection regardless of seizure phenotype. Notably, LEfSe analysis further indicates loss of genus *Prevotella* in TMEV-infected rodents, mirroring published findings at acute timepoints in TMEV-infected SJL mice.[27] Additionally, TMEV-infection

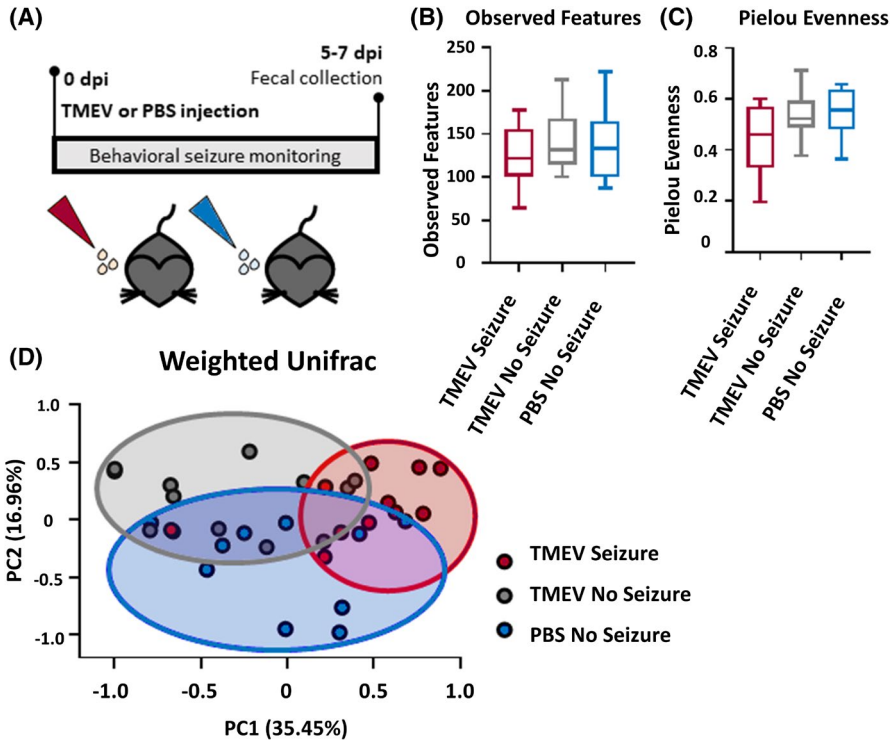

FIGURE 1 Theiler murine encephalomyelitis virus (TMEV) infection and seizure phenotype are associated with shifts in gut microbiome diversity. (A) Timeline of TMEV infection, behavioral seizure monitoring, and fecal collection for 16S sequencing. TMEV–seizure, $n = 11$ mice; TMEV–no seizure, $n = 12$ mice; phosphate-buffered saline (PBS)–no seizure, $n = 11$ mice. (B) Alpha diversity measured via observed features (not significant using Kruskal–Wallis *H*-test). (C) Alpha diversity measured via evenness index ($p = .08$ using Kruskal–Wallis *H*-test). (D) Beta diversity measured via weighted UniFrac distance (permutational multivariate analysis of variance, $p = .001$). dpi, days postinfection; PC, principal component

reduced the abundance of genus *Bifidobacterium*. Together, these findings indicate that TMEV infection leads to specific alterations in the composition of the gut microbiota regardless of seizure phenotype.

3.3 | Seizure phenotype following TMEV infection is associated with loss of key microbes

As we are interested specifically in the link between seizure phenotype and gut microbe alterations, we aimed to identify microbial biomarkers of seizure phenotype. LEfSe analysis of TMEV-infected mice stratified by seizure phenotype identified genus *Lactobacillus* in class Bacilli as well as Streptococcaceae bacterium *RF32* as biomarkers of seizure phenotype following TMEV infection (Figure 3A,B). In contrast, phyla Tenericutes, classes Bacteroidia and Mollicutes, and genera *Roseburia*, *Anaeroplasma*, *Ruminococcus*, and *Adlercreutzia* are identified as biomarkers of TMEV-infected mice that do not develop acute seizures. Currently there are few mechanistic links between gut microbiome populations and seizure susceptibility. Given that gut microbes produce a variety of metabolites known to have widespread CNS targets,[28] we performed a thorough literature search to identify metabolites produced by the hallmark taxonomies identified in our LEfSe analyses. The majority of the taxonomies underrepresented in TMEV-infected mice with seizure phenotypes contained genera associated with the production of the bacterial metabolite S-equol (Table 1).[29–35] Specifically, genus *Adlercreutzia* (in family Coriobacteriaceae) currently only contains one species: *A. equolifaciens*, a relatively understudied gut microbe known to produce S-equol from dietary daidzein.[33] Considering that S-equol crosses the blood–brain barrier[13] and has been shown to reduce glutamate excitotoxicity in cultured neurons,[36] we next evaluated the effect of exogenous S-equol on neuronal physiology.

3.4 | S-Equol alters cortical neuronal physiology in naïve rodents

Few studies have previously examined the effects of exogenous S-equol in vitro at timescales appropriate for acute slice experiments.[37] As 300 μmol·L^{-1} exogenous S-equol has been shown to acutely alter calcium signaling in GLUTag cells,[38] we first examined the effects of 300 μmol·L^{-1} S-equol on cortical principal neuron firing properties and action potential threshold (Figure 4A,B). Whole cell patch-clamp

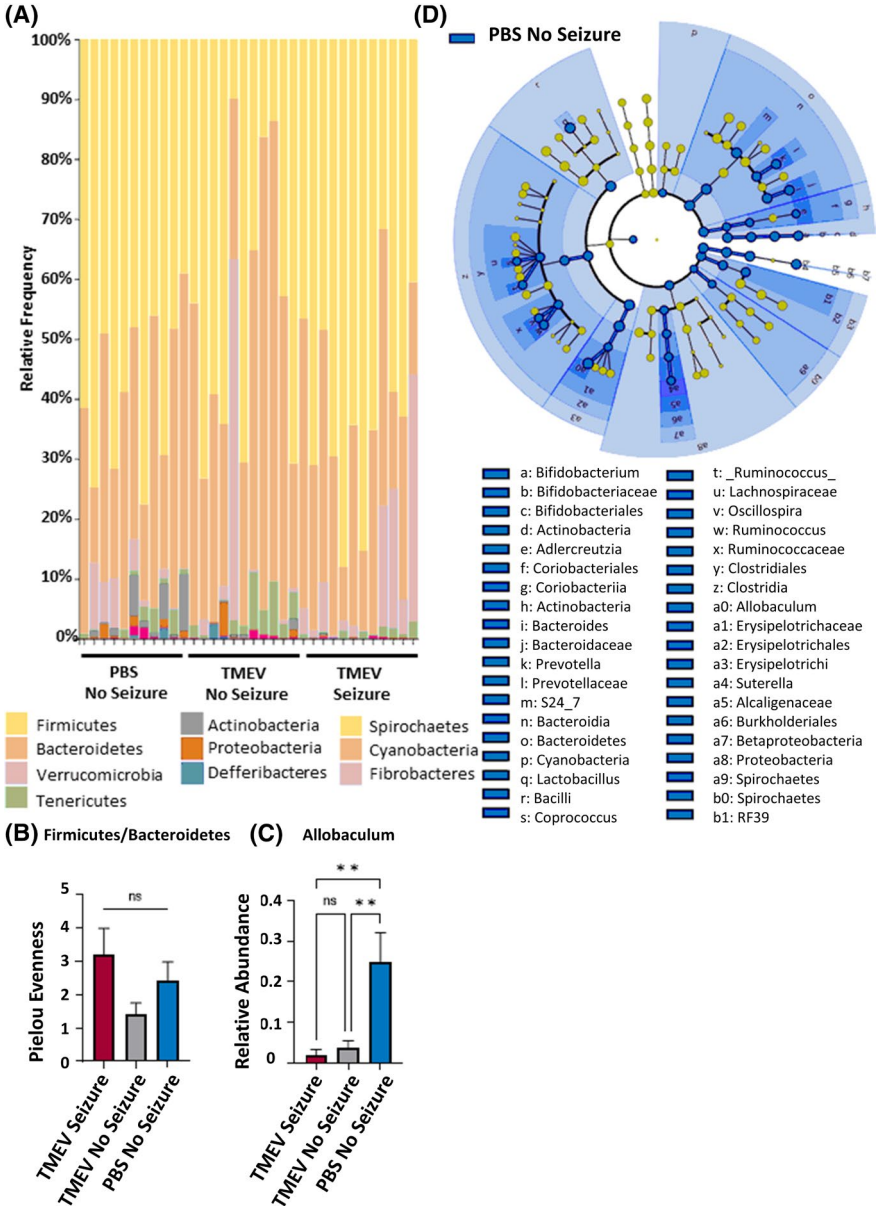

FIGURE 2 Theiler murine encephalomyelitis virus (TMEV) infection is associated with specific changes in gut microbes. (A) Relative abundance taxa bar plot showing bacteria phyla represented in each sample. (B) Firmicutes/Bacteroidetes ratio (not significant [ns]). (C) Relative abundance of *Allobaculum* genus. Analysis of compositions of microbiomes (ANCOM) result: null hypothesis rejected. $^{**}p < .01$ via Kruskal–Wallis *H*-test with Dunn multiple comparison analysis. (D) Functional characterization of operational taxonomic units (OTUs) represented in the gut microbiota of phosphate-buffered saline (PBS)-injected mice compared TMEV-infected mice. Significant OTUs have been identified by linear discriminant analysis (LDA) in addition to effect size. Significance is represented by LDA > 2

recordings were obtained from visually identified layer 2/3 pyramidal neurons in naïve adult male mice. Short current injections with 2-pA incremental increase in amplitude were used to determine changes in action potential current threshold. Thirty-minute exogenous application of high S-equol (300 μmol·L^{-1}) concentration increased the action potential firing threshold (ACSF, 193.111 ± 24.26 pA; 300 μmol·L^{-1} S-equol, 260.4 ± 29.08 pA; $p = .0102$, Student paired *t*-test; Figure 4A). Next, action potentials were elicited with 1-s-long current injections of increasing amplitude, and the effect of 300 μmol·L^{-1} S-equol was tested. We found that 300 μmol·L^{-1} S-equol decreased the number of action potentials following increasing current injection steps (ACSF vs. 300 μmol·L^{-1} S-equol, $p = .0001$, repeated measures two-way ANOVA with Bonferroni correction for comparisons; Figure 4B) without altering the resting membrane potential (RMP) of cortical neurons (ACSF, −64.33 ± 5.2 mV; 300 μmol·L^{-1} S-equol, −60.01 ± 11.55 mV; ns, Student paired *t*-test; Figure 4C).

Although in vitro literature on S-equol ranges in concentrations up to 300 μmol·L^{-1},[38,39] in vivo S-equol treatment in mice has only been shown to lead to serum S-equol concentrations approaching 10 μmol·L^{-1}.[40] We next examined the effect of 10 μmol·L^{-1} S-equol on the function of neurons from naïve male mice. A lower concentration of S-equol (10 μmol·L^{-1}) also increased the action potential firing threshold (ACSF, 232.5 ± 101.7 pA; 10 μmol·L^{-1} S-equol, 289.4 ± 101.3 pA; $p = .0026$, Student paired *t*-test; Figure 4D), and decreased the number of action potentials following increasing current injection, although to a lesser extent than a high dose of S-equol (ACSF vs. 10 μmol·L^{-1} S-equol, $p = .0003$, repeated measures two-way ANOVA with Bonferroni correction for comparisons; Figure 4E), but did not alter the RMP (ACSF, −68.11 ± 3.0 mV; 10 μmol·L^{-1}

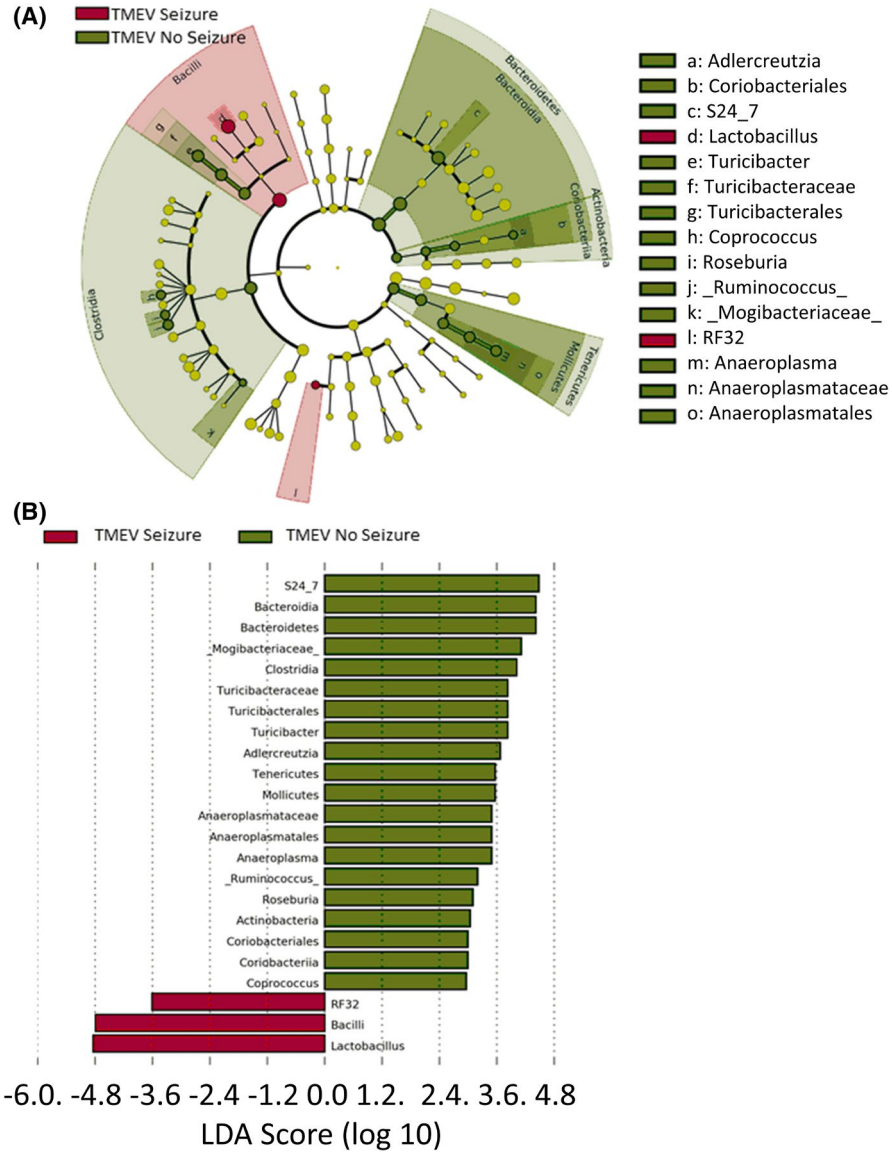

FIGURE 3 Seizure phenotype following Theiler murine encephalomyelitis virus (TMEV) infection is associated with alterations in gut microbes. Functional characterization of operational taxonomic units (OTUs) represented in the gut microbiota of TMEV-infected mice is stratified by seizure phenotype. Significant OTUs have been identified by linear discriminant analysis (LDA) in addition to effect size (LEfSe). Significance is represented by LDA > 2. (A) Cladogram of biomarkers identified in LEfSe analysis. (B) Histogram of LDA scores of taxonomies identified in LEfSe analysis. Green histograms represent biomarkers of TMEV-infected mice with no seizures. Red histograms represent biomarkers of TMEV-infected mice with seizure phenotypes

S-equol, −66.8 ± 9.758 mV; ns, Student paired *t*-test; Figure 4F). These results demonstrate concentration-dependent alterations in neuronal firing properties following 30-min exposure to exogenous S-equol.

As exogenous S-equol has previously been shown to exert a time-dependent effect in vitro,[39] we lastly preincubated acute slices from naïve male mice in 1 μmol·L^{-1} S-equol for more than 2 h to examine the effects of prolonged S-equol exposure at low levels. Preincubation of 1 μmol·L^{-1} S-equol increased the action potential firing threshold (ACSF, 130.6 ± 34.36 pA; 1 μmol·L^{-1} S-equol, 195.8 ± 71.42 pA; $p = .0168$, Student *t*-test; Figure 4G). Preincubation with 1 μmol·L^{-1} S-equol led to a trend toward a decrease in the number of action potentials, but this did not reach significance (ACSF vs. 1 μmol·L^{-1} S-equol, ns, repeated measures two-way ANOVA with Bonferroni correction for comparisons; Figure 4H) and the RMP was also not changed (ACSF, −65.06 ± 2.2 mV; 1 μmol·L^{-1} S-equol, −68.39 ± 2.24 mV; ns, Student *t*-test; Figure 4I). Together, these data demonstrate that S-equol alters cortical neuronal physiology in a concentration and time-dependent manner.

3.5 | Microbially derived metabolite S-equol ameliorates TMEV-induced ECTX hyperexcitability

As our microbiome data showed the loss of S-equol producing bacterial in TMEV–seizure mice and S-equol decreased basal neuronal activity, we set out to examine the effect of S-equol on neuronal excitability in TMEV-infected mice with seizures. S-equol (1 μmol·L^{-1}) application in ex vivo brain slices significantly increased the action potential firing threshold of ECTX neurons from acute slices collected at 5–7 dpi from male and female TMEV-infected mice with confirmed behavioral seizure phenotypes (PBS, 174.35 ± 12.7

TABLE 1 Mean relative abundances of key taxonomies identified via LEfSe analysis of TMEV-infected mice stratified by seizure phenotype

Taxonomy	TMEV–no seizure, mean relative abundance	TMEV–seizure, mean relative abundance	Equol-producing status
Bacteroidetes[a]	4.40E-01	2.71E-01	Zhang et al. 2012 (correlated with equol levels)
Bacteroidia	4.40E-01	2.71E-01	n/a
S24_7	3.16E-01	1.31E-01	n/a
Mogibacteriaceae	2.36E-04	5.94E-05	n/a
Clostridia[a]	1.58E-01	5.47E-02	Ge et al. 2020
Turicibacteraceae	5.71E-02	1.34E-02	n/a
Turicibacter	5.71E-02	1.34E-02	n/a
Actinobacteria[a]	3.31E-03	5.60E-04	Reviewed in Mayo et al. 2019, Clavel et al. 2014
Coriobacteriia[a]	1.68E-03	2.62E-04	Reviewed in Clavel et al. 2014
Adlercreutzia[a]	8.55E-04	2.42E-04	Maruo et al. 2008; reviewed in Clavel et al. 2014
Coriobacteriales[a]	1.68E-03	2.62E-04	Reviewed in Clavel et al. 2014
Mollicutes	2.96E-02	8.12E-03	n/a
Anaeroplasmataceae	1.89E-02	7.06E-04	n/a
Anaeroplasmatales	1.89E-02	7.06E-04	n/a
Anaeroplasma	1.89E-02	7.06E-04	n/a
Roseburia	2.17E-03	1.89E-04	n/a
Ruminococcus[a]	8.61E-03	2.62E-03	Guadamuro et al. 2019, Guadamuro et al. 2015 (correlated with equol levels)
Coprococcus[a]	1.92E-03	1.05E-03	Guadamuro et al. 2019 (correlated with equol levels)
Tenericutes	2.96E-02	8.12E-03	n/a

Abbreviations: LEfSe, linear discriminant effect size analysis; n/a, not available; TMEV, Theiler murine encephalomyelitis virus.

[a]Taxonomies lower in abundance in TMEV-infected mice with seizure phenotypes that are associated with equol production.

pA; TMEV–seizure, 113.25 ± 8.6 pA; TMEV–seizure + 1 μmol·L^{-1} S-equol, 166.72 ± 13.6 pA; PBS + 1 μmol·L^{-1} S-equol, 226.7 ± 82.67 pA; $p = .0001$, one-way ANOVA with Tukey multiple comparisons; Figure 5A). This effect is not due to changes in the RMP, as it was not different between neurons from TMEV-infected mice and controls (PBS mean = −61.5 ± 1.3 mV; TMEV–seizure, −62.9 ± 1.8 mV; TMEV–seizure + 1 μmol·L^{-1} S-equol, −61.2 ± 2.3 mV; PBS + 1 μmol·L^{-1} S-equol, −66.66 ± 4.76 mV; ns, one-way ANOVA; Figure 5B). Furthermore, TMEV infection altered the input–output curve of ECTX neurons following current injection (Figure 5C). Neurons from PBS controls displayed typical input–output curves with increasing numbers of action potentials with increasing current injection. In contrast, neurons from TMEV-infected mice showed higher excitability by firing more action potentials at lower current injection compared to PBS control. In response to higher current injections (>150 pA), neurons from TMEV-infected mice displayed a depolarization block (Figure 5C), a silent state of a neuron in response to excessive excitation.[41] In contrast, 1 μmol·L^{-1} S-equol application prevents the depolarization block observed in ECTX neurons from TMEV-infected mice, and decreases the number of action potentials fired in neurons from PBS-injected mice at 120-pA current injection (PBS vs. TMEV vs. TMEV + S-equol vs. PBS + S-equol, $p = 0001$, repeated measures two-way ANOVA with Bonferroni correction for comparisons; Figure 5C). Taken together, these findings indicate that S-equol can ameliorate TMEV-induced hyperexcitability in ECTX neurons.

4 | DISCUSSION

In the present study, we show significant alterations in the gut microbiome of C57BL/6J mice following TMEV infection. Additionally, we identify key microbial taxa associated with TMEV-induced seizure phenotype. We demonstrate the ability of exogenous S-equol to alter neuronal physiology in a dose- and time-dependent manner. Lastly, we also show marked alterations in neuronal physiology in the ECTX of TMEV-infected mice, and demonstrate the ability of microbially derived S-equol to ameliorate TMEV-induced

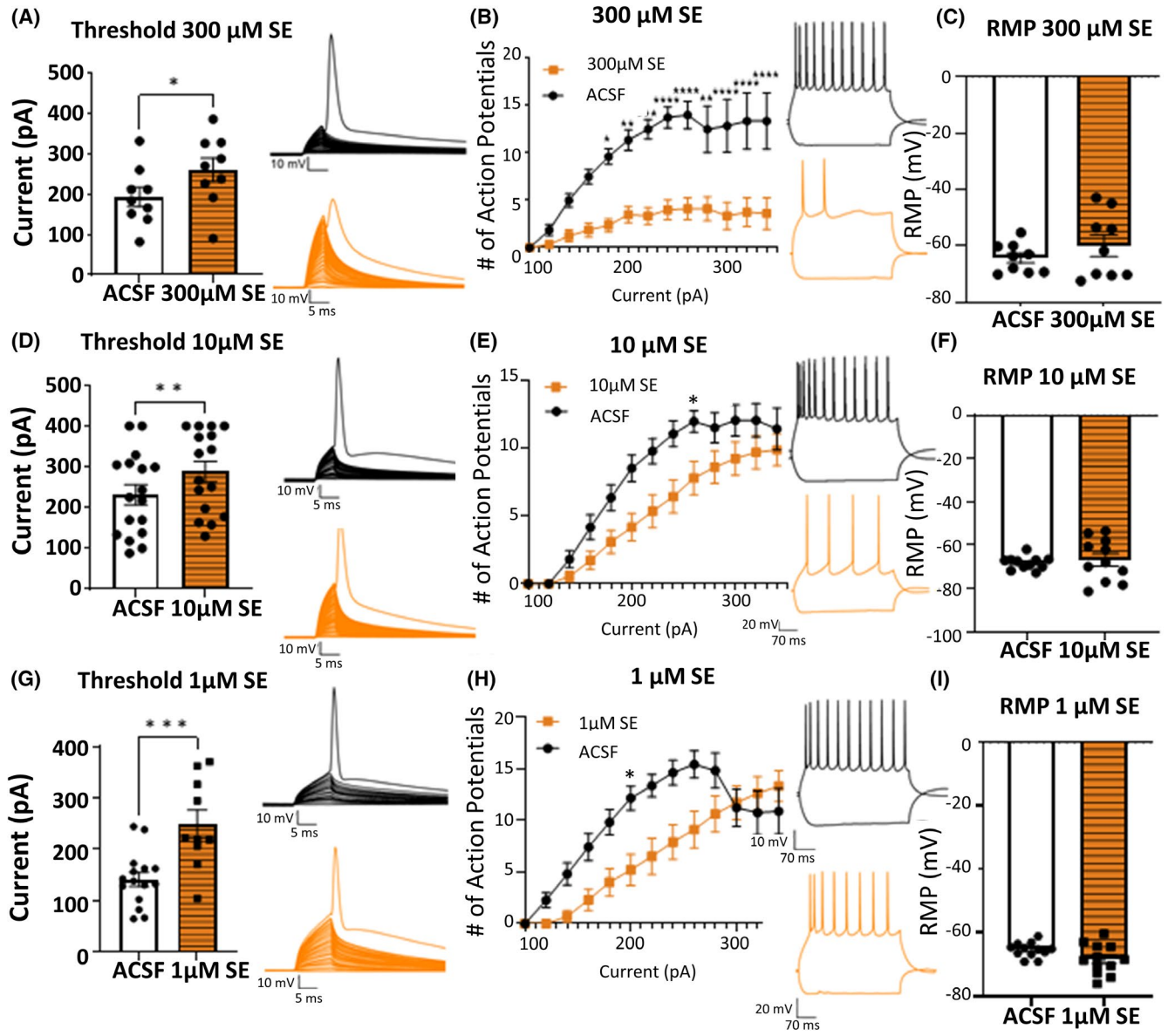

FIGURE 4 Exogenous S-equol (SE) alters naïve neuronal physiology in a concentration- and time-dependent manner. (A) Threshold to fire first action potential following current injection at 2-pA steps before and after 30-min 300-µmol·L^{-1} S-equol wash. *$p < .05$ using Student *t*-test. (B) Input–output curve of number of action potentials following current injection at 20-pA steps before and after 30-min 300-µmol·L^{-1} S-equol wash. *$p < .05$, **$p < .01$, ***$p < .001$, ****$p < .00001$ using two-way analysis of variance (ANOVA). Representative traces at 100-pA current injection are shown. (C) Resting membrane potential (RMP) before and after 30-min 300-µmol·L^{-1} S-equol wash (not significant [ns] using Student *t*-test.). (D) Threshold to fire first action potential following current injection at 2-pA steps before and after 30-min 10-µmol·L^{-1} S-equol wash. **$p < .01$ using Student *t*-test. (E) Input–output curve of number of action potentials following current injection at 20-pA steps before and after 30-min 10-µmol·L^{-1} S-equol wash. *$p < .05$ using two-way ANOVA. Representative traces at 100-pA current injection are shown. (F) RMP before and after 30-min 10-µmol·L^{-1} S-equol wash (ns using Student *t*-test). (G) Threshold to fire first action potential following current injection at 2-pA steps following preincubation in 1 µmol·L^{-1} S-equol. *$p < .05$ using Student *t*-test. (H) Input–output curve of number of action potentials following current injection at 20 pA following preincubation in 1 µmol·L^{-1} S-equol (ns using two-way ANOVA). Representative traces at 100-pA current injection are shown. (I) RMP following preincubation in 1 µmol·L^{-1} S-equol (ns using Student *t*-test). ACSF, artificial cerebrospinal fluid

hyperexcitability. Collectively, our results indicate a central role for a microbially derived metabolite in regulating neuronal excitability and propose a mechanistic link between the gut–brain axis and virus-induced seizures.

In our study, ANCOM analysis revealed significant reduction of genus *Allobaculum* in the microbiomes of TMEV-infected mice. Interestingly, *Allobaculum* has been associated with 5-hydroxytryptamine levels in a mouse model of depression,[42]

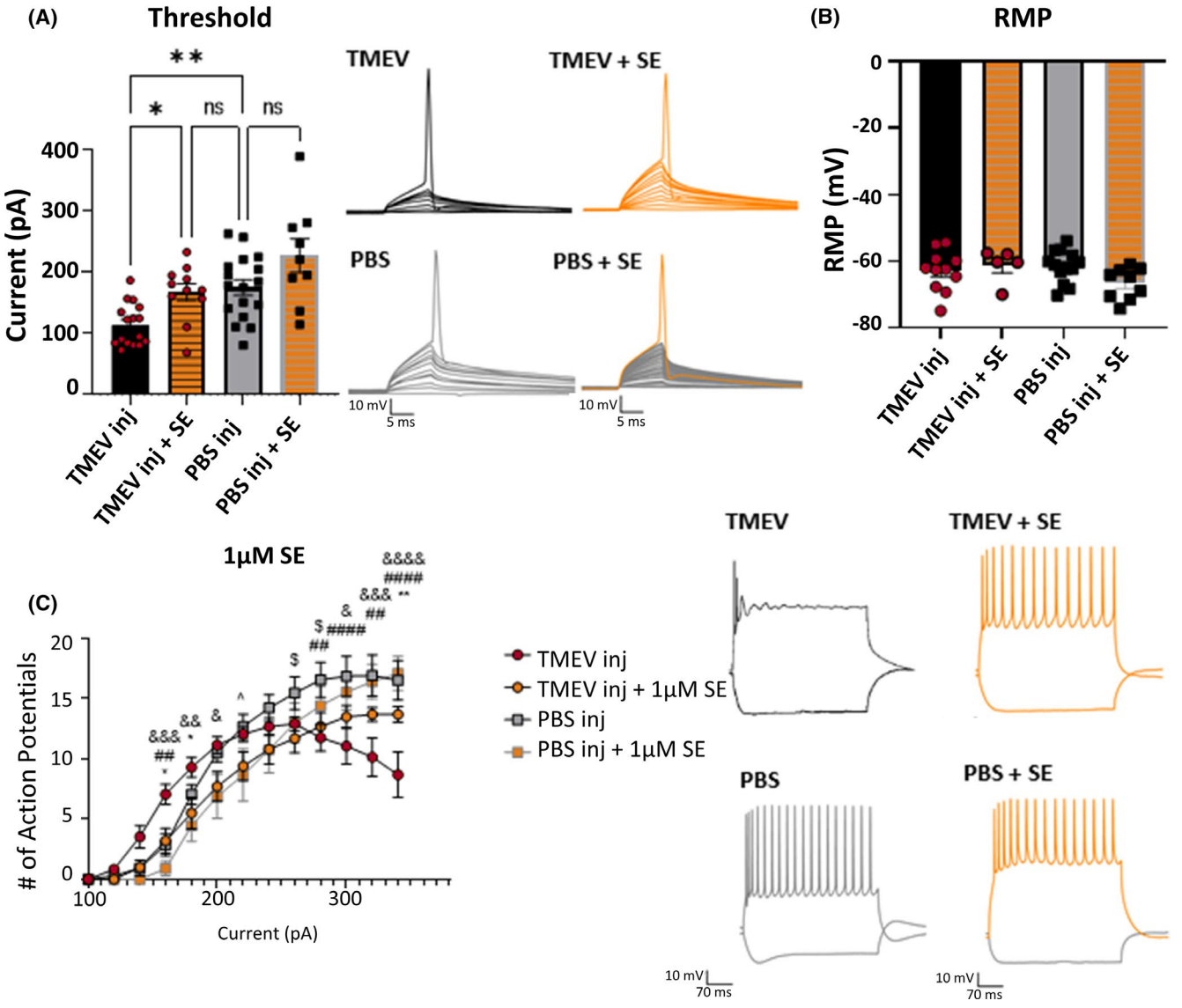

FIGURE 5 Exogenous S-equol (SE) reduces Theiler murine encephalomyelitis virus (TMEV)-induced neuronal hyperexcitability. (A) Threshold to fire first action potential following current injection (inj) at 2-pA steps. $^{*}p < .05$, $^{**}p < .01$. ns, not significant. (B) Resting membrane potential (RMP; ns using Kruskal–Wallis *H*-test). (C) Input–output curve of number of action potentials following current injection at 20-pA steps. Difference between TMEV and TMEV + 1 µmol·L^{-1} SE: $^{*}p < .05$, $^{**}p < .01$; difference between TMEV and phosphate-buffered saline (PBS): $^{\#\#}p < .01$, $^{\#\#\#\#}p < .0001$; difference between TMEV and PBS + 1 µmol·L^{-1} SE: $^{\&}p < .05$, $^{\&\&}p < .01$, $^{\&\&\&}p < .001$, $^{\&\&\&\&}p < .0001$; difference between PBS and PBS + 1 µmol·L^{-1} SE; $^{\$}p < .05$ difference between TMEV + 1 µmol·L–1 SE and PBS + 1 µmol·L–1 SE: $^{\wedge}p < .05$ using two-way analysis of variance. Representative traces at 240-pA current injection are shown

and was similarly reduced in a mouse model of schizophrenia,[43] indicating a potential role for loss of *Allobaculum* in neurological disease. LEfSe analysis additionally revealed loss of genus *Adlercreutzia* in TMEV-infected mice with seizure phenotypes. Genus *Adlercreutzia* currently only contains one species: *A. equolifaciens*, a bacterial species known to produce S-equol.[33] S-Equol is a gut microbial metabolite of dietary isoflavone daidzein, which can be found in soy and other plant products, that is highly able to permeate the gut and the blood–brain barrier.[13] The neuroprotective effects of equol are well documented.[36] However, no study has previously examined the effect of S-equol on neuronal physiology.

Loss of CA1 hippocampal neurons and altered neuronal physiology in CA3 and dentate gyrus neurons is a hallmark of TMEV-associated seizures.[44] Additionally, there is widespread cortical astrogliosis following TMEV injection, indicating the presence of cortical pathogenesis alongside classical hippocampal pathogenesis. The entorhinal cortex has long been a structure of interest in the pathogenesis of temporal lobe epilepsy (TLE)[45]; however, no study has examined electrophysiological properties of ECTX neurons following TMEV infection. In the current study, we demonstrated that ECTX neurons from TMEV-infected mice with seizure phenotypes have a reduced threshold to fire an action

potential following current injection, and display prominent depolarization block at high levels of sustained current injection. Excitingly, we show that exogenous application of microbial metabolite S-equol (1 μmol·L^{-1}) ameliorates TMEV-induced ECTX neuronal hyperexcitability.

TLE patients often experience a disease progression consisting of an initial insult,[46] followed by a highly variable quiescent period during which massive cellular alterations occur,[47] and finally the onset of chronic seizures.[48] Many rodent models of epilepsy, including TMEV, follow a similar disease progression.[25] Probiotics have been shown to be beneficial in rodent models during the initial insult phase of TLE, reducing the occurrence of acute seizures following pentylenetetrazole (PTZ)-induced kindling[8] and 6-Hz stimulation,[7] and in a genetic model of absence seizures.[49] Microbiota transplant is additionally protective in rodents against PTZ-induced seizures following chronic stress.[50] Regarding chronic seizures, adults with drug-resistant chronic seizures have altered microbiomes, and probiotic supplementation has been shown to improve seizure burden in adults with refractory chronic seizures.[6,9] Probiotic therapy has also been shown to reduce chronic seizure burden in a *Kcna1*$^{-/-}$ rodent model of epilepsy.[7] The current study provides evidence for microbiome alteration at an acute-disease timepoint (5–7 dpi) following intracranial TMEV infection in mice. As the gut–brain axis is bidirectional, where disease states can influence microbial populations and in turn, microbes can alter disease states via complex systemic pathways, a limitation of the current study is that no directional link can be drawn between TMEV-induced seizures and the described microbiome alterations at 5–7 dpi. Future studies are necessary to elucidate the possibility of complex, bidirectional interactions of TMEV infection, seizure phenotype, and microbiome alterations. The current study further provides evidence of a potential therapeutic benefit of exogenous S-equol during the acute phase of TMEV-induced seizures. Given that there is evidence for microbiota involvement in chronic seizures in both rodents and humans, it is possible that S-equol will also be beneficial during epileptogenesis and chronic epilepsy phases. More studies are necessary to elucidate the involvement of the gut microbiota and S-equol beyond acute seizure periods.

Taken together, our results demonstrate a clear role of the gut–brain axis in TMEV-induced seizures. These data highlight the role of S-equol and the gut–brain axis in virus-induced seizures and identify a new target in the study of gut–brain axis therapeutics in epilepsy.

ACKNOWLEDGMENTS

This work was partly supported by the Virginia Tech Institute for Critical Technology and Applied Science and startup funds from the College of Agricultural and Life Sciences and the School of Neuroscience at Virginia Tech to S.L.C. Sequencing was performed at the Genomics Sequencing Center, which is part of the Fralin Life Science Institute at Virginia Tech (FLSI-illuminaseq@vt.edu 540-231-1229).

CONFLICT OF INTEREST

None of the authors has any conflict of interest to disclose. We confirm that we have read the Journal's position on issues involved in ethical publication and affirm that this report is consistent with those guidelines.

ORCID

Susan L. Campbell https://orcid.org/0000-0001-7775-8600

REFERENCES

1. World Health Organization. Epilepsy: a public health imperative. 2019. http://www.who.int/mental_health/neurology/epilepsy/report_2019/en/. Accessed 11 Jan 2021.
2. De Caro C, Leo A, Nesci V, Ghelardini C, di Cesare ML, Striano P, et al. Intestinal inflammation increases convulsant activity and reduces antiepileptic drug efficacy in a mouse model of epilepsy. Sci Rep. 2019;9(1):13983.
3. Dahlin M, Prast-Nielsen S. The gut microbiome and epilepsy. EBioMedicine. 2019;44:741–6.
4. Lum GR, Olson CA, Hsiao EY. Emerging roles for the intestinal microbiome in epilepsy. Neurobiol Dis. 2020;135:e104576.
5. Zhang Y, Zhou S, Zhou Y, Yu L, Zhang L, Wang Y. Altered gut microbiome composition in children with refractory epilepsy after ketogenic diet. Epilepsy Res. 2018;145:163–8.
6. Peng A, Qiu X, Lai W, Li W, Zhang L, Zhu X, et al. Altered composition of the gut microbiome in patients with drug-resistant epilepsy. Epilepsy Res. 2018;147:102–7.
7. Olson CA, Vuong HE, Yano JM, Liang QY, Nusbaum DJ, Hsiao EY. The gut microbiota mediates the anti-seizure effects of the ketogenic diet. Cell. 2018;173(7):1728–41.e13.
8. Bagheri S, Heydari A, Alinaghipour A, Salami M. Effect of probiotic supplementation on seizure activity and cognitive performance in PTZ-induced chemical kindling. Epilepsy Behav. 2019;1(95):43–50.
9. Gómez-Eguílaz M, Ramón-Trapero JL, Pérez-Martínez L, Blanco JR. The beneficial effect of probiotics as a supplementary treatment in drug-resistant epilepsy: a pilot study. Benef Microbes. 2018;9(6):875–81.
10. Iannone LF, Gómez-Eguílaz M, Citaro R, Russo E. The potential role of interventions impacting on gut-microbiota in epilepsy. Expert Rev Clin Pharmacol. 2020;13(4):423–35.
11. Setchell KDR, Clerici C, Lephart ED, Cole SJ, Heenan C, Castellani D, et al. S-equol, a potent ligand for estrogen receptor beta, is the exclusive enantiomeric form of the soy isoflavone metabolite produced by human intestinal bacterial flora. Am J Clin Nutr. 2005;81(5):1072–9.
12. Nagel SC, vom Saal FS, Welshons WV. The effective free fraction of estradiol and xenoestrogens in human serum measured by whole cell uptake assays: physiology of delivery modifies estrogenic activity. Proc Soc Exp Biol Med. 1998;217(3):300–9.
13. Johnson SL, Kirk RD, DaSilva NA, Ma H, Seeram NP, Bertin MJ. Polyphenol microbial metabolites exhibit gut and blood–brain barrier permeability and protect murine microglia against LPS-induced inflammation. Metabolites. 2019;9(4):78.

14. Rowland IR, Wiseman H, Sanders TA, Adlercreutz H, Bowey EA. Interindividual variation in metabolism of soy isoflavones and lignans: influence of habitual diet on equol production by the gut microflora. Nutr Cancer. 2000;36(1):27–32.
15. Thom M. Review: Hippocampal sclerosis in epilepsy: a neuropathology review. Neuropathol Appl Neurobiol. 2014;40(5):520–43.
16. Sommer W. Erkrankung des Ammonshorns als aetiologisches Moment der Epilepsie. Arch Für Psychiatr Nervenkrankh. 1880;10(3):631–75.
17. Patel DC, Wallis G, Fujinami RS, Wilcox KS, Smith MD. Cannabidiol reduces seizures following CNS infection with Theiler's murine encephalomyelitis virus. Epilepsia Open. 2019;4(3):431–42.
18. Racine RJ. Modification of seizure activity by electrical stimulation: II. Motor seizure. Electroencephalogr Clin Neurophysiol. 1972;32(3):281–94.
19. Bolyen E, Rideout JR, Dillon MR, Bokulich NA, Abnet CC, Al-Ghalith GA, et al. Reproducible, interactive, scalable and extensible microbiome data science using QIIME 2. Nat Biotechnol. 2019;37(8):852–7.
20. Mandal S, Van Treuren W, White RA, Eggesbø M, Knight R, Peddada SD. Analysis of composition of microbiomes: a novel method for studying microbial composition. Microb Ecol Health Dis. 2015;26(s3):27663–70.
21. Segata N, Izard J, Waldron L, Gevers D, Miropolsky L, Garrett WS, et al. Metagenomic biomarker discovery and explanation. Genome Biol. 2011;12(6):R60.
22. Alcoreza O, Tewari BP, Bouslog A, Savoia A, Sontheimer H, Campbell SL. Sulfasalazine decreases mouse cortical hyperexcitability. Epilepsia. 2019;60(7):1365–77.
23. Ting JT, Lee BR, Chong P, Soler-Llavina G, Cobbs C, Koch C, et al. Preparation of acute brain slices using an optimized N-methyl-D-glucamine protective recovery method. J Vis Exp. 2018;(132):53825.
24. Tewari BP, Chaunsali L, Campbell SL, Patel DC, Goode AE, Sontheimer H. Perineuronal nets decrease membrane capacitance of peritumoral fast spiking interneurons in a model of epilepsy. Nat Commun. 2018;9(1):4724.
25. Stewart K-AA, Wilcox KS, Fujinami RS, White HS. Development of postinfection epilepsy after Theiler's virus infection of C57BL/6 mice. J Neuropathol Exp Neurol. 2010;69(12):1210–9.
26. Mandal S, Treuren WV, White RA, Eggesbø M, Knight R, Peddada SD. Analysis of composition of microbiomes: a novel method for studying microbial composition. Microb Ecol Health Dis. 2015;26(1):27663.
27. Carrillo-Salinas FJ, Mestre L, Mecha M, Feliú A, Del Campo R, Villarrubia N, et al. Gut dysbiosis and neuroimmune responses to brain infection with Theiler's murine encephalomyelitis virus. Sci Rep. 2017;14(7):44377.
28. Zeng X, Hu K, Chen L, Zhou L, Luo W, Li C, et al. The effects of ginsenoside compound K against epilepsy by enhancing the γ-aminobutyric acid signaling pathway. Front Pharmacol. 2018;9:1020.
29. Zhang X, Zheng W, Huang S, Yao W. Microbial conversion of daidzein affects fecal equol concentration and bacterial composition of rats with or without ovariectomy. Wei Sheng Wu Xue Bao. 2012;52(7):866–74.
30. Ge Y-F, Wei C-H, Wang W-H, Cao L-K. The effect of sorghum resistance resistant starch-mediated equol on the histological morphology of the uterus and ovaries of postmenopausal rats. Food Sci Nutr. 2020;8(8):4055–65.
31. Mayo B, Vázquez L, Flórez AB. Equol: a bacterial metabolite from the daidzein isoflavone and its presumed beneficial health effects. Nutrients. 2019;11(9):2231.
32. Clavel T, Lepage P, Charrier C. The family Coriobacteriaceae. In: Rosenberg E, DeLong EF, Lory S, Stackebrandt E, Thompson F, editors. The prokaryotes: Actinobacteria. Berlin, Heidelberg: Springer; 2014. p. 201–38.
33. Maruo T, Sakamoto M, Ito C, Toda T, Benno Y. Adlercreutzia equolifaciens gen. nov., sp. nov., an equol-producing bacterium isolated from human faeces, and emended description of the genus Eggerthella. Int J Syst Evol Microbiol. 2008;58(5):1221–7.
34. Guadamuro L, Azcárate-Peril MA, Tojo R, Mayo B, Delgado S. Use of high throughput amplicon sequencing and ethidium monoazide dye to track microbiota changes in an equol-producing menopausal woman receiving a long-term isoflavones treatment. AIMS Microbiol. 2019;5(1):102–16.
35. Guadamuro L, Delgado S, Redruello B, Flórez AB, Suárez A, Martínez-Camblor P, et al. Equol status and changes in fecal microbiota in menopausal women receiving long-term treatment for menopause symptoms with a soy-isoflavone concentrate. Front Microbiol. 2015;6:777.
36. Zhao L, Chen Q, Diaz BR. Neuroprotective and neurotrophic efficacy of phytoestrogens in cultured hippocampal neurons. Exp Biol Med (Maywood). 2002;227(7):509–19.
37. Buskila Y, Breen PP, Tapson J, van Schaik A, Barton M, Morley JW. Extending the viability of acute brain slices. Sci Rep. 2014;4(1):5309.
38. Harada K, Sada S, Sakaguchi H, Takizawa M, Ishida R, Tsuboi T. Bacterial metabolite S-equol modulates glucagon-like peptide-1 secretion from enteroendocrine L cell line GLUTag cells via actin polymerization. Biochem Biophys Res Commun. 2018;501(4):1009–15.
39. Moriyama M, Hashimoto A, Satoh H, Kawabe K, Ogawa M, Takano K, et al. S-Equol, a major isoflavone from soybean, inhibits nitric oxide production in lipopolysaccharide-stimulated rat astrocytes partially via the GPR30-mediated pathway. Int J Inflam. 2018;2018:8496973.
40. Selvaraj V, Zakroczymski MA, Naaz A, Mukai M, Ju YH, Doerge DR, et al. Estrogenicity of the isoflavone metabolite equol on reproductive and non-reproductive organs in mice. Biol Reprod. 2004;71(3):966–72.
41. Kim CM, Nykamp DQ. The influence of depolarization block on seizure-like activity in networks of excitatory and inhibitory neurons. J Comput Neurosci. 2017;43(1):65–79.
42. Wu M, Tian T, Mao Q, Zou T, Zhou C-J, Xie J, et al. Associations between disordered gut microbiota and changes of neurotransmitters and short-chain fatty acids in depressed mice. Transl Psychiatry. 2020;10(1):350.
43. Gubert C, Kong G, Uzungil V, Zeleznikow-Johnston AM, Burrows EL, Renoir T, et al. Microbiome profiling reveals gut dysbiosis in the metabotropic glutamate receptor 5 knockout mouse model of schizophrenia. Front Cell Dev Biol. 2020;8:e582320.
44. Buenz EJ, Sauer BM, Lafrance-Corey RG, Deb C, Denic A, German CL, et al. Apoptosis of hippocampal pyramidal neurons is virus independent in a mouse model of acute neurovirulent picornavirus infection. Am J Pathol. 2009;175(2):668–84.
45. Gloveli T, Schmitz D, Heinemann U. Interaction between superficial layers of the entorhinal cortex and the hippocampus in normal and epileptic temporal lobe. Epilepsy Res. 1998;32(1):183–93.

46. Mathern GW, Adelson PD, Cahan LD, Leite JP. Hippocampal neuron damage in human epilepsy: Meyer's hypothesis revisited. Prog Brain Res. 2002;135:237–51.
47. Dudek FE, Hellier JL, Williams PA, Ferraro DJ, Staley KJ. The course of cellular alterations associated with the development of spontaneous seizures after status epilepticus. Prog Brain Res. 2002;135:53–65.
48. French JA, Williamson PD, Thadani VM, Darcey TM, Mattson RH, Spencer SS, et al. Characteristics of medial temporal lobe epilepsy: I. Results of history and physical examination. Ann Neurol. 1993;34(6):774–80.
49. Citraro R, Lembo F, De Caro C, Tallarico M, Coretti L, Iannone LF, et al. First evidence of altered microbiota and intestinal damage and their link to absence epilepsy in a genetic animal model, the WAG/Rij rat. Epilepsia. 2021;62(2):529–41.
50. Medel-Matus J-S, Shin D, Dorfman E, Sankar R, Mazarati A. Facilitation of kindling epileptogenesis by chronic stress may be mediated by intestinal microbiome. Epilepsia Open. 2018;3(2):290–4.

How to cite this article: Gallucci A, Patel DC, Thai K, Trinh J, Gude R, Shukla D, et al. Gut metabolite S-equol ameliorates hyperexcitability in entorhinal cortex neurons following Theiler murine encephalomyelitis virus-induced acute seizures. *Epilepsia*. 2021;00:1–13. https://doi.org/10.1111/epi.16979